View metadata, citation and similar papers at core.ac.uk
brought to you by CORE
provided by CiteSeerX

November 11-15, 2007, Seattle, Washington, USA

IMECE2007-43403

# COMPUTATIONAL STUDY OF SIC HALIDE CHEMICAL VAPOR DEPOSITION SYSTEM

**Rong Wang, Ronghui Ma**
**Department of Mechanical Engineering**
**University of Maryland, Baltimore County – UMBC**
**Baltimore, MD 21250**

**Govindhan Dhanaraj, Yi Chen and Michael Dudley**
**Department of Materials Science and Engineering**
**Stony Brook University**
**Stony Brook, NY 11794**

## ABSTRACT
Halide CVD (HCVD) is recently employed to grow SiC epitaxial layers using $SiCl_4/C_3H_8/H_2$ mixtures in an effort to achieve high deposition rates. The introduction of the chlorinated species allows the formation of more stable species $SiCl_2$ while maintaining high surface reactivity, thus avoiding the silicon gas phase nucleation that has been widely reported in conventional CVD process using $SiH_4/C_3H_8/H_2$. However, the difficulties in reducing defect density and controlling the electrical properties of the material present a significant technical obstacle for HCVD of SiC. In experimental growth, the electrical properties, defect densities and the growth rate of as-deposited SiC epitaxial films are, to a large extent, determined by processing parameters including temperature, pressure, flow rates of precursors and carrier gas. Optimization of growth conditions provides the opportunity to engineer films with desired film properties and qualities at high deposition rate but requires in-depth understanding the deposition process. In this study, we performed computational study to investigate the effects of main processing parameters in HCVD process on film growth. Numerical experiments were performed over a wide range of operational parameters to provide information on distributions of gas velocity, temperature, and chemical species' concentrations in the reactor as well as the deposition rates on the substrate surface. Simulations were also carried out to address hot zone design and operational conditions.

## INTRODUCTION
Silicon carbide is an attractive semiconductor material to construct electronic devices functioning under extreme conditions such as high temperatures, high power, and erosive environments [1]. Most of these devices are fabricated on epitaxial layers grown by chemical vapor deposition (CVD) method. Historically, silane and propane highly diluted in hydrogen carrier gas are extensively used as precursors in CVD of SiC [2-7]. However, low deposition rate (3 to 15 $\mu m/h$) renders it not economically cost-effective for devices requiring thick SiC epilayers (100 $\mu m$). Recently, research effort has been made towards an alternative approach, halide CVD process, to grow thick SiC epilayers using silicon tetrachloride ($SiCl_4$) and propane as precursors [8,9]. Whilst high deposition rate in the range of 50 – 250 $\mu m/h$ has been achieved, some technical issues such as defect densities and material properties need to be addressed.

Experimental growth shows that the properties of the film are dependent on the processing parameters, such as deposition temperature and input gas flow rates [9]. However, it is difficult to identify adequate processing conditions for growing film of specific characteristics without advanced understanding of the deposition mechanism. Numerical simulation provides an inexpensive and expedient means to study the growth process. In this study, we developed a comprehensive modeling framework for a hot wall horizontal reactor that involves gas phase reaction, surface chemistry, transport of mass, momentum and energy, and electromagnetic dynamics. Specifically, the gas phase reaction and surface kinetics were incorporated into transport model, thus enabling the prediction of the flow field, thermal condition and deposition rates under wide range of processing conditions and reactor configurations. Special attention was directed to the study of the effects of deposition temperature and various flow rates of precursors, $C_3H_8$ and $SiCl_4$, on the growth rate and C/Si ratio in the system.

## NOMENCLATURE
$T$ = temperature
$\rho$ = density of the gas mixture
$\mathbf{v}$ = velocity
$p$ = pressure
$\mathbf{g}$ = gravitational acceleration
$\mu$ = viscosity
$I$ = identity tensor
$h$ = enthalpy
$k$ = thermal conductivity
$Q$ = heating source
$D$ = diffusion coefficient of species
$Y$ = mass fraction
$i$ = species index
$\dot{\omega}$ = reaction rate
$\boldsymbol{A}$ = magnetic vector potential
$\boldsymbol{J}_{coil}$ = current density in coil


Copyright © 2007 by ASME

| | | |
|---|---|---|
| $q'''_{eddy}$ | = | heat power generated by eddy current |
| $\gamma$ | = | sticking coefficient |
| $\varepsilon_m$ | = | relative permittivity |
| $\mu_m$ | = | relative permeability |
| $\sigma_c$ | = | electrical conductivity |
| *Gr* | = | Grashof number |
| *Re* | = | Reynolds number |

## I. Experimental Study

SiC thick epilayers were grown in a CVD system at Stony Brook University [10] as schematically shown in Fig. 1 using silicon tetrachloride ($SiCl_4$) and propane ($C_3H_8$) diluted in hydrogen ($H_2$). Commercially available 6H on-axis SiC wafers produced by physical vapor transport (PVT) were cut into 1 cm by 1 cm size seeds and served as substrates. The substrate was situated on a tilted graphite plate ($0 \sim 15^o$) in order to achieve uniform thickness. The growth was performed at temperature ranging from 1400 to 1700°C with the flow rates of silicon tetrachloride, propane and hydrogen being 30-120 sccm, 10-20 sccm and 5-15 slm, respectively. The epilayer thickness was calculated by the measuring weight increase as well as by observing the cross-sectional view under the Nomarski microscope.

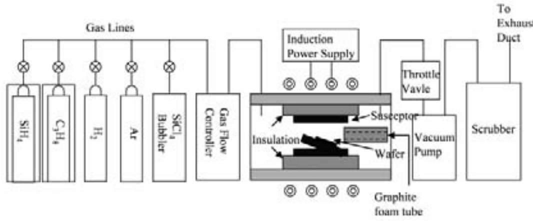


**Figure 1: Schematic diagram of HCVD system.**

## II. Mathematical Model

**Transport processes:** The fluid flow, heat and mass transfer in the reactor are governed by the conservation of momentum, thermal energy, individual and total mass. The model assumes the reactor is axisymmetric and operated under steady state during film growth. The gas flow is assumed to be laminar and the viscous dissipation of the gas mixture is neglected. The gas mixture is treated as ideal gas and is transparent for radiation. The radiation heat transfer within the system is also considered using the surface-to-surface radiation method. Based on flow rates and operational parameters used in experimental growth, the $Gr/Re^2$, with a physical interpretation of the ratio of buoyancy forces to inertial forces, is estimated to be very small, which indicates buoyancy induced flow can be neglected in the simulation. Thus the governing equations of transport processes are given as:

$$\nabla \cdot (\rho \mathbf{v}) = 0 \tag{1}$$

$$\rho \mathbf{v} \cdot \nabla \mathbf{v} = -\nabla p + \nabla \cdot \{\mu[\nabla \mathbf{v} + (\nabla \mathbf{v})^T] - \frac{2}{3}\mu \mathbf{I} \nabla \cdot \mathbf{v}\} + \rho \mathbf{g} \tag{2}$$

$$\nabla \cdot (\rho \mathbf{v} h) = \nabla \cdot (k \nabla T) + Q \tag{3}$$

$$\nabla \cdot (\rho \mathbf{v} Y_i) = \nabla \cdot (\rho D \nabla Y_i) + \dot{\omega}_i \tag{4}$$

where $\rho$ is the density of the gas mixture, $\mathbf{v}$ is the velocity, $p$ is the pressure, $\boldsymbol{g}$ is the gravitational acceleration, $\mu$ is viscosity, $\boldsymbol{I}$ is the identity tensor, $h$ is the enthalpy, $k$ is the thermal conductivity, $Q$ is the heating source term, and subscript $i$ denotes species i. In Eq. (4), $D$ is the binary diffusion coefficients of reactants in carrier gases, $Y$ and $\dot{\omega}_i$ are the mass fraction and gas generation rate of species $i$, respectively. $\dot{\omega}_i$ is calculated from gas phase chemistry.

The boundary conditions include constant gas flow velocity at the inlet. The deposition pressure is 200 Torr. The inlet gas is considered to be at the room temperature, so is the outer surface of the insulation because it is in contact with double-walled quartz tube cooled by water at room temperature. A detailed description of this mathematical model can be found in our previous publication [11].

**Induction heating:** Induction heating has been widely used to achieve deposition temperature beyond 1500°C in the HCVD system required for high growth rate. The magnitude and distribution of Joule's heating are determined by the hot zone design and induction heating parameters such as the frequency, input power, position and geometry of the coils. In current study, the volumetric Joule's heating Q in Eq. (2) is calculated by solving Maxwell's equation. At low frequency (less than 1MHz), it is assumed that the electromagnetic field is quasi-steady and axis-symmetric, and the current in the coils is time harmonic. The Maxwell's equation in terms of magnetic vector potential is given as:

$$\nabla \times (\frac{1}{\mu_m} \nabla \times \mathbf{A}) + \varepsilon_m \frac{\partial^2 \mathbf{A}}{\partial t^2} + \sigma_c \frac{\partial \mathbf{A}}{\partial t} = \mathbf{J}_{coil} \tag{5}$$

The generated heating by eddy current in the graphite susceptor is calculated using Joule's law:

$$q'''_{eddy} = \frac{1}{2} \sigma_c \omega^2 (A_r^2 + A_i^2) \tag{6}$$

The model assumes the magnetic potential diminishes at the infinite distance from the coils.

**Gas phase reaction:** To our knowledge, the existing analysis and modeling works were developed based on gas phase equilibrium analysis. A complete kinetic mechanism for reactions in $SiCl_4/H_2/C_3H_8$ is not available and information in this aspect at high temperature is quite limited. In current study, a comprehensive reaction mechanism is proposed including one set of reactions for the $C_3H_8$ decomposition, one set for $SiCl_4$ decomposition, and one set of reaction among products from the first two sets. Considering the large number of reactions, including all the possible reaction steps and chemical species in the simulation is very difficult, if not impossible, due to the high demand in computational resource. A selection of reactions and species has been made based on equilibrium analysis. The kinetic mechanism employed in the model involves 76 reactions and 33 species. The details of description of the construction of the reaction mechanism can be found in our previous work [11].

 Copyright © 2007 by ASME

**Surface deposition of SiC:** Currently a widely used method to model the surface deposition in a CVD process is sticking coefficient method, which assumes the deposition process is transport limited when temperature is high. However, because of the high gas flow rates, high species concentrations and high deposition rates involved in a SiC HCVD process, the hypothesis of transport limited growth may not hold. In this study, we employed a kinetic surface deposition model involves 9 surface species and 29 reactions [11] that include complex deposition processes such as gas species adsorptions, surface species reactions, film etching, and film formation.

**Etching of graphite susceptor:** In the HCVD system, the graphite etching can be substantial as evidenced by the low flow rate of propane in the experimental growth [9,10]. Contrary to SiC deposition from $SiH_4$ in which the C/Si ratio in the precursors is maintained above or close to unity [2-7], the C/Si ratio in the precursors in HCVD process can be as low as 0.2 [10]. Considering the higher probabilities of Si species to be deposited on the substrate than C species, this low C/Si ratio implies that graphite etching provides a substantial source of carbon, and therefore, has a significant impact on the gas phase composition and stoichiometry. A multi-step mechanism for graphite etching by hydrogen atoms at temperature higher than 1000K proposed by Balooch and Olander [12] is used in this study.

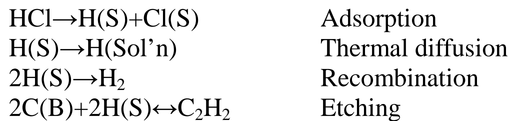

| | |
|---|---|
| $HCl \rightarrow H(S)+Cl(S)$ | Adsorption |
| $H(S) \rightarrow H(Sol'n)$ | Thermal diffusion |
| $2H(S) \rightarrow H_2$ | Recombination |
| $2C(B)+2H(S) \leftrightarrow C_2H_2$ | Etching |

## III. Simulation Configuration

Numerical simulations are performed in a two-dimensional, axisymmetrical configuration with the identical dimensions as the experimental growth. The simulated growth chamber consists of a dense graphite susceptor enclosed in a tubular graphite foam as shown schematically in Fig. 2. A SiC substrate of 1cm×1cm is positioned on the susceptor wall. The growth chamber sealed in quartz tube is heated by radio frequency induction heating system. The mixture of the precursors and carrier gas is delivered from the left end of the chamber and exhausted from the other outlet. The simulation assumes the reactor is operated under 200 Torr as described in experimental work. The distributions of temperature, gas velocity, species' concentrations in the reactor chamber are predicted through solving equations for electromagnetic dynamics and reaction kinetics in coupling with equations for conservation of energy, momentum, and mass. The simulations are performed using the commercial software package CFD-ACE with a mesh system of 349×133. The grid dependence of the results has been examined using a refined grid system and consistent results have been produced.

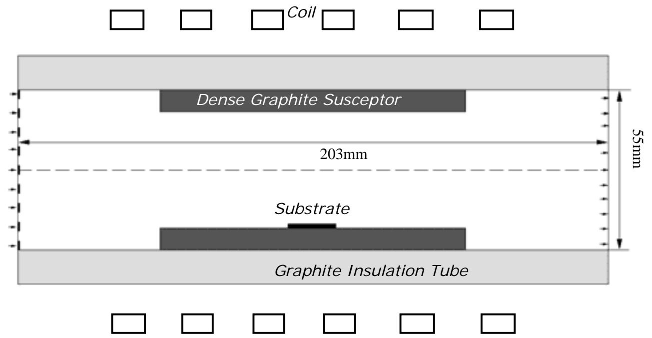


**Figure 2: Schematics of simulated reactor hot zone for SiC HCVD system.**

## IV. Results and Discussions

**Electromagnetic field and Joule heating:** The induction heating process is modeled by solving Maxwell's equation for the electromagnetic field, followed by applying Joule's law to calculate the heat generation in the dense graphite susceptor by eddy current. Fig. 3 and Fig. 4 present magnetic vector potential distributions in the reactor and the heat generation distribution in the susceptor at frequency of 25 Khz, current of 350 A. Due to the skin effect of induction heating, more heat is localized in the outer layer of the susceptor.

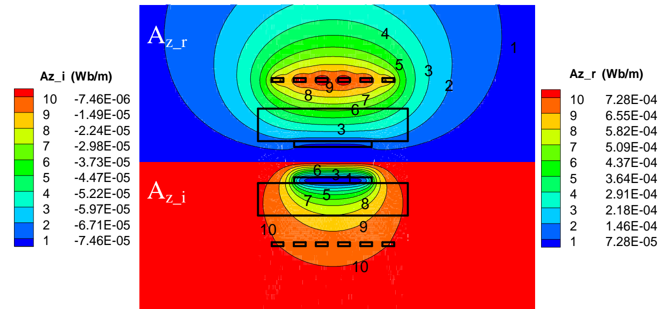


**Figure 3: Distributions of in-phase ($A_r$) and out-of-phase ($A_i$) components of magnetic vector potential.**

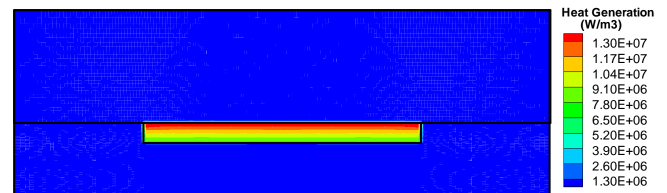


**Figure 4: Heat distribution in the susceptor generated by the eddy current.**

**Flow field and temperature profile:** The flow field and the temperature distribution inside the reactor were studied by solving the conservation of mass, momentum and energy coupled with induction heating. Shown in Fig. 5 is the calculated laminar flow field and corresponding temperature profile. The highest temperature is observed in the wall of the graphite susceptor at the axial center of the tube. This can be


Copyright © 2007 by ASME

explained by the fact that heating is mainly produced by eddy current induced within the dense graphite susceptor of high electric conductivity. Since the inlet gas temperature is much lower than that in the hot zone, there exists a temperature difference approximately 200 K across the susceptor in the axial direction. The high temperature in the hot zone facilitates multiple chemical reactions in gas phase and on the surface of substrate. To fully understand the deposition mechanism, it is necessary to model the gas phase decomposition process and identify the important species.

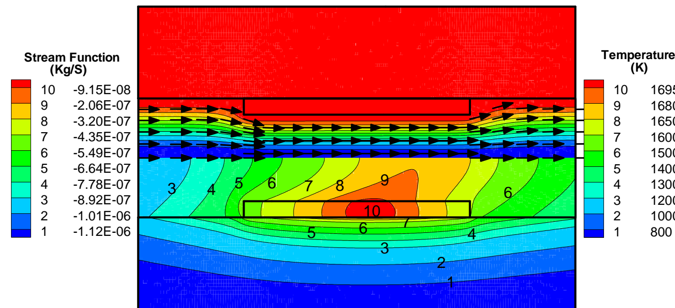


**Figure 5: Flow field and temperature distribution in the reactor at 1700K.**

**Species concentration:** The pyrolysis of precursors was studied by incorporating the gas phase and surface chemistry into the transport model. Specifically, the graphite etching and film etching were considered in this calculation. Shown in Fig. 6 are molar concentrations of important species along the axial centerline of the susceptor. Fig. 6(a) shows the Si-bearing species concentrations. It can be seen that, at this temperature, $SiCl_4$ decomposes rapidly into $SiCl_2$, SiCl and $SiH_xCl_y$, among which $SiCl_2$ is the most important species with the highest concentration observed in the system. Fig. 6(b) presents the hydrocarbon species concentrations. It shows that $CH_4$ is the dominant C-bearing species in the reactor.

The gas species' concentrations on the substrate surface are of special interest because they directly affect the rate of surface reactions, and subsequently determine the deposition rate. As shown in Fig. 7, the species' concentrations over the substrate surface are different from those in Fig. 6 because of the occurrence of the surface deposition. Worth noticing are the high concentration levels of SiCl and CH resulting from etching of the film by HCl:

$$SiC(B)+HCl \rightarrow SiCl+CH$$

The abundance of HCl in the current system is mainly produced by the reaction:

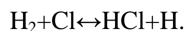

$$H_2+Cl \leftrightarrow HCl+H.$$

It is also observed in Fig. 7 that at the substrate surface, the concentrations of atom Cl and H are also high. This is believed to relate to the hydrocarbon and $SiCl_2$ adsorptions. When the adsorption reactions occur, the Si and C atoms are incorporated into the film, the H and Cl atoms are released into the gas phase, producing HCl by the reactions of $SiCl_2 \rightarrow SiCl(S)+Cl$ and $CH_4 \rightarrow C(S)+H_2$.

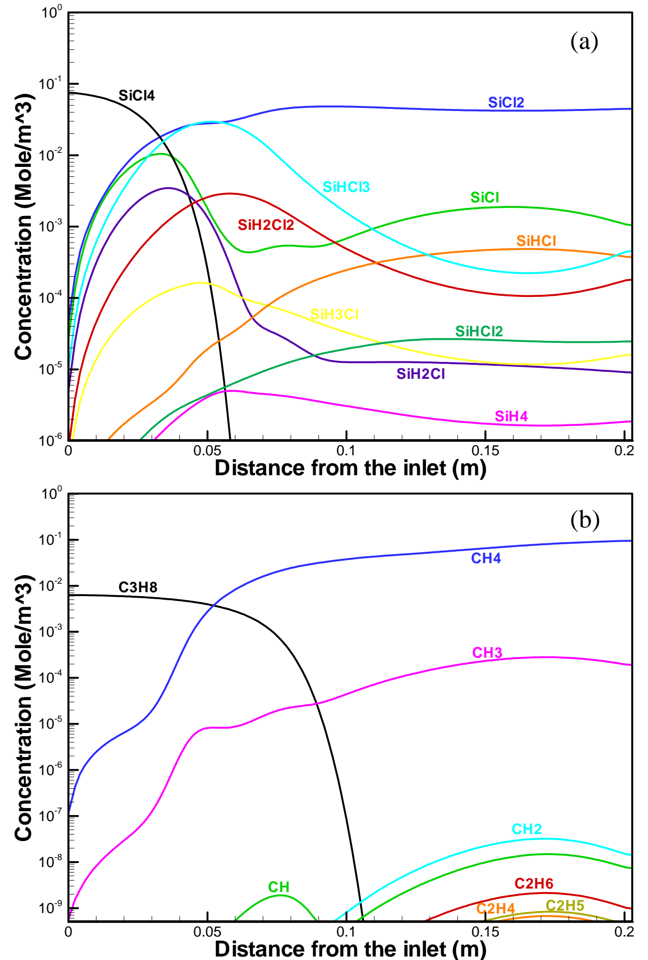


**Figure 6: Molar concentrations of main species in the axial direction at 1700K: (a) Si-bearing species; (b) C-bearing species.**

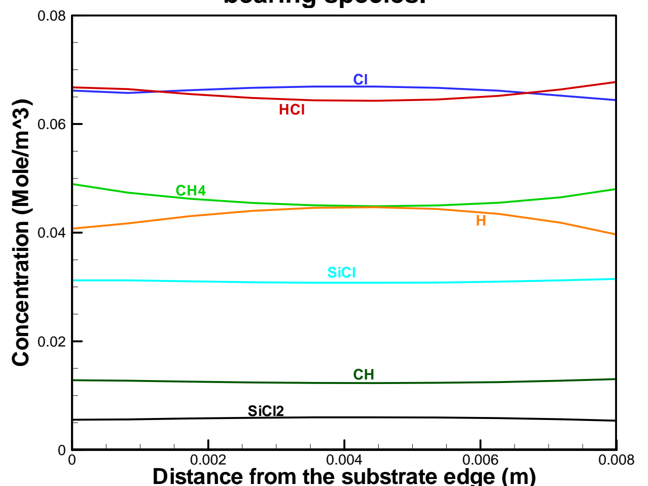


**Figure 7: Molar concentrations of main species on the substrate surface at 1700K.**


Copyright © 2007 by ASME

**Effect of temperature on deposition rate:** The growth of the SiC film was modeled at the deposition temperature ranging from 1400°C to 1700°C with the flow rates of $SiCl_4$, $C_3H_8$ and $H_2$ being 120 sccm, 10 sccm, and 5000 sccm, respectively. The predicted deposition rates by kinetic model and experimental measurements [10] under identical conditions at various temperature agrees reasonably well as illustrated in Fig. 8. Importantly, the numerical prediction captures the decreasing trend of the deposition rates with increasing temperature, which agrees with thermodynamic equilibrium analysis. The reduced deposition rate with temperature can be explained by the etching of SiC film by HCl. As shown in Fig. 9, HCl concentration in the system increases monotonously with temperature, which in turns enhances the etching process and reduces the deposition rate. Deposition temperature also increases C/Si ratio in the system as illustrated in Fig. 10 because graphite etching on the graphite susceptor is temperature dependent. For all the cases, the C/Si is greater than unity.

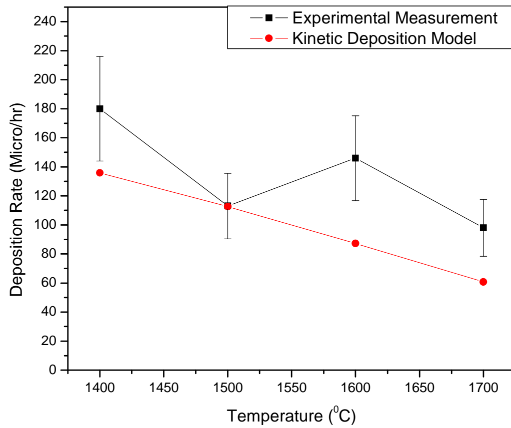


**Figure 8: Comparison of experimentally measured and predicted deposition rates at different temperatures.**

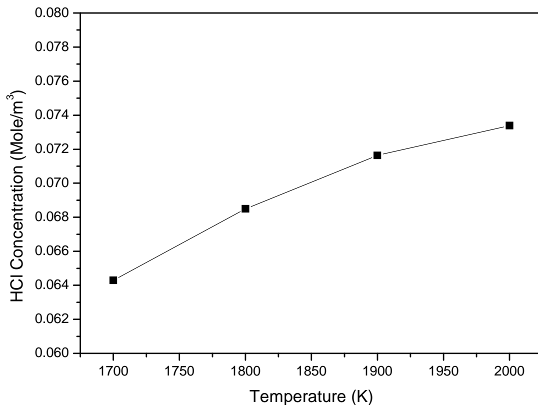


**Figure 9: HCl concentrations on the substrate surface for different deposition temperatures.**

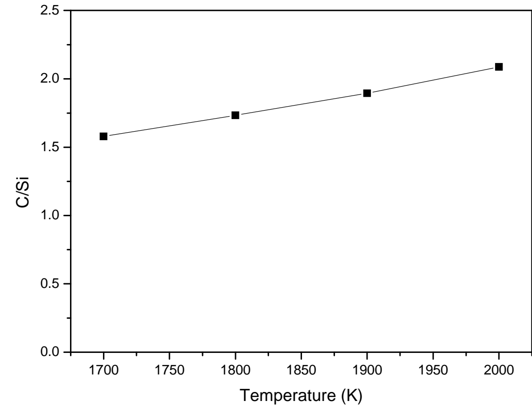


**Figure 10: C/Si ratios on the substrate surface at different deposition temperatures.**

**Effect of $C_3H_8$ flow rate:** The effect of $C_3H_8$ flow rate was studied by simulating the deposition process with $C_3H_8$ flow rate varied between 0 to 40 sccm at deposition temperature of 1700K. The $H_2$ and $SiCl_4$ flow rates were kept at 5000 sccm and 120 sccm, respectively. Fig. 11 shows the variation SiC growth rate as function of $C_3H_8$ flow rates. The dependence of the deposition rates on $C_3H_8$ flow rates is weak. As propane flow rate increases, the deposition rate first reaches its peak value followed by a decrease. This can be explained by the HCl etching mechanism in the furnace. HCl plays a very important role in the system including offering carbon source through graphite etching and reducing the film growth by surface etching. For deposition with the propane flow rate below 5 sccm, the carbon species concentration in the system is mainly provided by graphite etching by HCl, which consumes HCl and graphite, releasing $C_2H_2$ and $Cl_2$ gas. With propane flow rated being elevated, the increase in carbon species concentration tends to reduce the rates of graphite etching process, which subsequently reduces the rate of HCl consumption. As a result, HCl concentration increases with $C_3H_8$ flow rate, leading to enhanced film etching and reduced deposition rate.

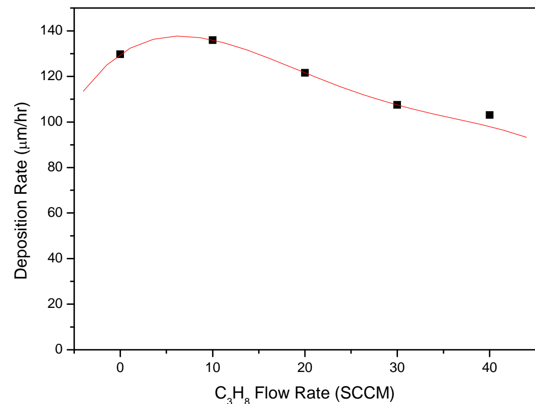


**Figure 11: Deposition rates as a function of $C_3H_8$ flow rates at 1700K.**


Copyright © 2007 by ASME

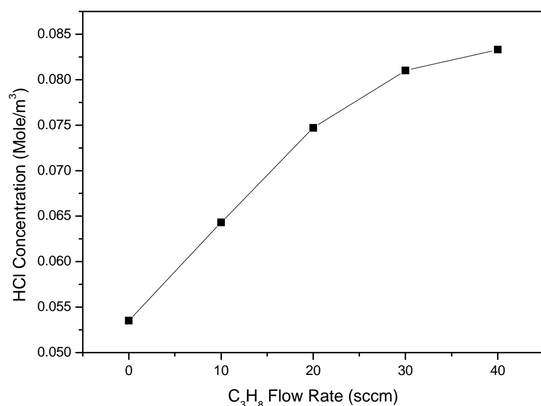


**Figure 12: HCl concentrations on the substrate as a function of $C_3H_8$ flow rates at 1700 K.**

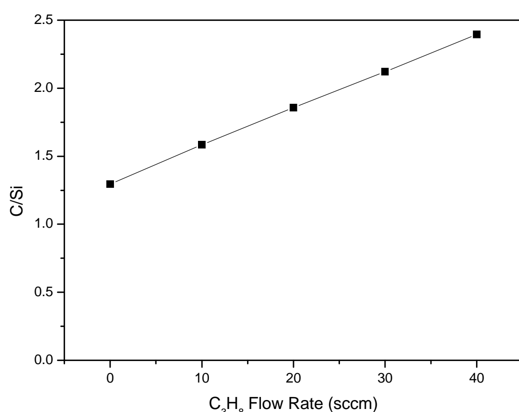


**Figure 13: C/Si ratios on the substrate as a function of $C_3H_8$ flow rates at 1700K.**

Fig. 13 shows C/Si ratio increases quasi-linearly with propane flow rate. Interestingly, when no propane is provided, the C/Si ratio is still around unity, which illustrates that graphite etching provides substantial source of carbon in the current system. This result agrees with Balooch and Olander's analysis [12] that the propane only provides a small portion of hydrocarbon in the system and serves as the secondary source of carbon.

**Effect of $SiCl_4$ flow rate:** In order to determine the dependence of SiC growth rate on input flow rate of $SiCl_4$, simulations were performed with $H_2$ and $C_3H_8$ flow rates fixed at 10 and 5000 sccm, respectively, and $SiCl_4$ flow rate varied from 60-360 sccm. As shown in Fig. 14, the growth rate increases with $SiCl_4$ flow rate. This observation suggests the growth is Si-limited and addition in Si source leads to enhanced growth rate. Interestingly, the rate of growth rate increase slows down as $SiCl_4$ supply approaches 400 sccm. The corresponding variation of HCl concentration on the substrate surface with $SiCl_4$ flow rate as shown in Fig. 15 suggests an explanation. With high concentration of $SiCl_4$, the dissociation of $SiCl_4$ produces a large amount of Cl atoms, which react with $H_2$ and form HCl. Since the most significant consequence of the presence of HCl in the system is film etching, the increase in HCl concentration enhances film etching and increase in growth rate due to additional Si source is compromised.

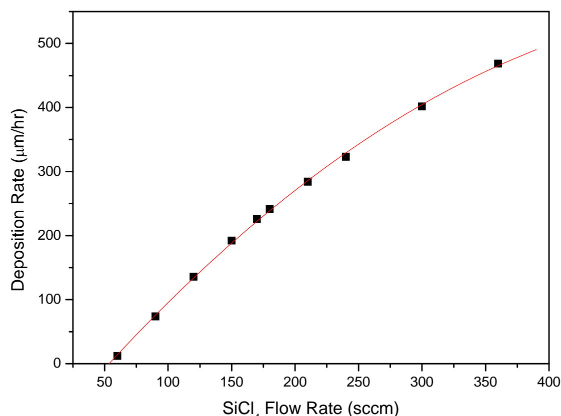


**Figure 14: Deposition rates as a function of $SiCl_4$ flow rates at 1700K.**

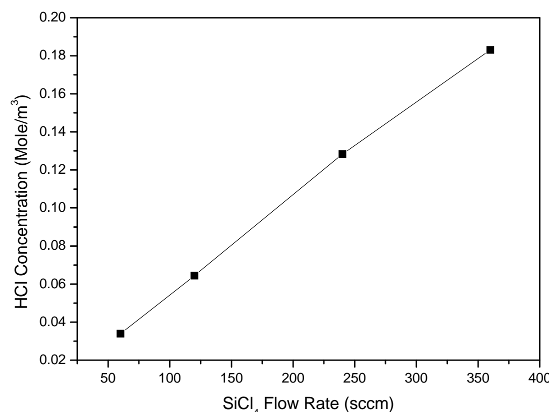


**Figure 15: HCl concentrations on the substrate as a function of $SiCl_4$ flow rates at 1700K.**

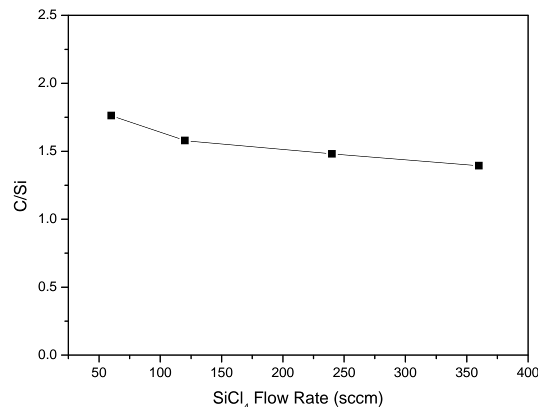


**Figure 16: C/Si ratios on the substrate as a function of $SiCl_4$ flow rates at 1700K.**


Copyright © 2007 by ASME

## V. Conclusion

A comprehensive model of SiC HCVD system using $SiCl_4/C_3H_8/H_2$ as precursor has been developed which includes transport processes, gas phase and surface kinetics, and electromagnetic dynamcis. The model is applied to a horizontal hot wall HCVD reactor to study SiC epilayer film growth process and flow rates of precursors. The deposition rates predicted by this model are compared with experimental measurements. It is illustrated the prediction agrees with the experimental growth. Further simulations of deposition are conducted under various growth conditions including deposition temperature, flow rates of $C_3H_8$ and $SiCl_4$. It is illustrated that HCl is an important species in graphite etching and film etching, thus, it plays an important role in determining the deposition rate. We also observe that under current growth system configuration, precise control of the gas composition and deposition rate is very difficult due to the graphite etching process. The modeling of the deposition process provides advanced understanding of the process as well as a solid base for judicious choice of deposition conditions.

## REFERENCES


[1] G. Dhanaraj, X. R. Huang, M. Dudley, V. Prasad and R. H. Ma, in: K. Byrappa, T. Ohachi (Eds.), *Crystal Growth Technology*, William Andrew co-published with Springer, NY, 2003, pp. 181-232 (Chapter 6).

[2] G. Wagner, D. Schulz, D. Siche, Prog. in *Crys. Grow. & Char. of Mater.*, 47 (2003) 139.

[3] A. Dollet, S. de Persis, M. Pons, M. Matecki, *Surf. & Coat. Tech.*, 177 (2004) 382

[4] A.N. Vorob'ev, S. Y. Karpov, M. V. Bogdanov, A. E. Komissarov, O. V. Bord, A. I. Zhmakin, Y. N. Makarov, *Comp. Mater. Sci.,* 24 (2002) 520.

[5] R. Rupp, A. Wiedenhofer, P. Friedrichs, D. Peters, R. Schorner, D. Stephani, *Silicon Carbide, III-Nitrides and Related Materials,* 264 (1998) 89.

[6] M. D. Allendorf, R. J. Kee, *J. Electro. Soc.,* 138 (1991) 841.

[7] O. Danielsson, A. Henry, E. Janzen, *J. Crystal Growth,* 243 (2002) 170.

[8] H. J. Chung, A. Y. Polyakov, S. W. Huh, S. Nigam, M. Skowronski, M. A. Fanton, B. E. Weiland, D. W. Snyder, *J. Appl. Phys.,* 97 ( 2005) 084913

[9] S. Nigam, H. J. Chung, A. Y. Polyakov, M. A. Fanton, B. E. Weiland, D. W. Snyder, M. Skowronski, *J. Crystal Growth,* 284 (2005) 112.

[10] Y. Chen, G. Dhanaraj, H. Chen, M. Dudley, and H. Zhang, *Mater. Res. Soc. Symp. Proc.* 891 (2005) EE12.09

[11] R. Wang, R. Ma, Kinetics of Halide Chemical Vapor Deposition of Silicon Carbide Film, *J. Crystal Growth,* (2007) Submitted.

[12] M. Balooch, D.R. Olander, *J. Chem. Phys.,* 63 (1975) 4



Copyright © 2007 by ASME